High Performance Disturbance Observer based Control of the Nonlinear 2DOF Helicopter System

Almir Salihbegovic, Emir Sokic, Nedim Osmic and Mujo Hebibovic
Department for Automatic Control and Electronics
Faculty of Electrical Engineering, University of Sarajevo
71000 Sarajevo, Bosnia and Herzegovina
almir.salihbegovic@etf.unsa.ba

Abstract— **This paper addresses the challenges of the disturbance observer (DOB) algorithms faced with highly nonlinear electromechanical systems which are dealing with high resolution and high speed operations. It describes the synthesis of robust and stable controllers and their applications in controlling azimuth and elevation angles of the helicopter model CE 150 supplied by Humosoft. Description of the helicopter, including its mechanical characteristics and mathematical model, is given in the paper. Tracking error, transient performances, power consumption and motor strains are used for the validation of control quality. Implementation of the control system on the experimental setup is also explained. MATLAB and Simulink are used as tools for developing the simulation model of the helicopter system. Obtained simulations are showing that developed controllers provide significantly improved results even in the presence of unknown and unpredictable inputs (disturbance and noise), unpredictable and unknown dynamics, external forces (torques) and change of the system parameters.**

I. Introduction

Modern electromechanical systems are often required to operate at high speeds to yield high productivity. Precision and accuracy requirements are becoming more and more strict at the same time. Advanced control plays a significant role while meeting these challenges.

The helicopters are widely used in transportation, air surveillance and as combat aerial vehicles. They are very interesting from the control point of view due to nonlinearity, instability in the open-loop and high cross-coupling effects. Main difficulties in controlling such systems are nonlinear friction, uncertainties of the systems parameters, unmodelled dynamics and external disturbances.

In the last two decades nonlinear control methods for the the nonlinear systems have been intensively developing [1]. For highly nonlinear systems usage of the classical control theory (PI, PD and PID controllers) is not recommended. These controllers give satisfactory results only in a very small area around the set point. The control performance could be improved using an output tracking based on approximate linearisation [2], [3]. This approach neglects cross-coupling effects of the helicopter. The model of a small unmanned helicopter has been linearised at different set points along the elevation axis and a gain scheduling control has been implemented in [4].

Many authors have been studied methods for controlling azimuth and elevation angles of the helicopter model CE 150 supplied by Humosoft [5]–[9]. The performance comparison of three optimal control techniques to a helicopter system: model predictive control (MPC), linear quadratic optimal control combined with a state estimator (LQG), and optimal linear quadratic output control (PLQ), is discussed in [8]. These three schemes obtained significantly improved results over classical control algorithms. However, the application of these algorithms is not trivial due to demand for frequent model linearisation and significant random disturbances. MPC has substantial inter-sample computation demands and the largest memory requirements [9]. LQG and PLQ algorithms proved satisfactory results only below the horizontal line $\psi = 0$. Above this angle the instability of the open loop plant and increasing model-plant mismatch leads to poor tracking results.

Papers [5]–[7] describe capabilities of the inteligent methods for controlling 2DOF nonlinear helicopter model. The fuzzy control in dealing with helicopter uncertainties is described in [5]. The capability of neural networks scheme to control laboratory helicopter model CE 150 was discussed in [6]. Performance of these controllers are slightly degraded due to inability for precise estimation of the helicopter parametric uncertainties, the dynamic of actuators, nonlinear friction forces, external disturbances and cross-coupling effects. Because of the computational burden of these algorithms, it is not efficient to implement these algorithms for the more complex realistic systems.

Design of disturbance observer (DOB) based controller is one of the most popular methods in the field of high performance positioning systems. DOB based techniques appeared in the late 1980s. In [10] dynamics for each elbow of the robot manipulator is decoupled, and DOB controller is designed for each part independently. The nonlinear disturbance observer based design, with assumed upper and lower bounds of the disturbance to be known, is discussed in [11]. The DOB based control has been widely used in industry [12]–[15]. This paper focuses on high performance tracking control for electrical driven helicopter body with unmodelled and unknown uncertainties. The cross-coupling effects of the elevation and azimuth dynamics can be treated as external disturbances. The DOB control is used to compensate these effects, thus the interference terms can be decoupled and the desired dynamics performances can be obtained. Hence, DOB and feed-forward control loop will be added to the PD feedback controller to improve robustness and tracking performance.

This paper is organized as follows. In Section II the helicopter system CE 150 is presented. Synthesis of the controllers in the acceleration framework is subject of Section III, describing the outer control loop of the cascade structure. This section also presents the inner control loop that realizes disturbance observer and its application in the control structures. Implementation of the control algorithm in simulation and experimental setup is discussed in Section IV. Concluding remarks are given in Section V.

II. Control System Description

The proposed real-time control system for the helicopter model is composed of three major components (as shown in Fig. 1): the PC based controllers, the interface module and the helicopter system. The PC based controllers of the elevation and azimuth angle are designed in MATLAB/Simulink. The multifunctional card MF624 is used as interface module between PC based controller and helicopter system. It is designed for data acquisition and transmission. The card is optimized for use with MATLAB/Simulink Real Time Toolbox. It also provides implementation of the control algorithms from the PC to the helicopter system. The MF624 card features fully 32 bit architecture for fast throughput. As the user communicates with the system via Real Time Toolbox interface, all input/output signals are dimensionless and scaled into the MU (Machine Unit) interval $\langle -1, +1 \rangle$. The MATLAB/Simulink xPC Target Toolbox is used to perform the experiments in real time applications. Finally, the helicopter system contains the helicopter body, two DC motors with permanent stator magnets, power amplifiers and encoders as sensors.

A. Model of the helicopter body

This subsection introduces the mathematical model of the helicopter CE 150 supplied by Humosoft Ltd. This model is used for synthesis of the controller and validating tracking performance. The helicopter is a rigid body with two DC motors that drive main and side rotors, power amplifiers and encoders as sensors. It has two degrees of freedom, elevation (pitch) angle ψ, that represent rotation around horizontal axis, and azimuth (jaw) angle φ, that represents rotation around vertical axis. The axis of main and side propellers are mutually orthogonal. The helicopter model is a MIMO system with two input signals (voltage of the main motor u_1 and voltage of the side motor u_2) and two output signals (elevation and azimuth), with operation ranges given in Table I.

TABLE I

Input and output signals of the helicopter model

	Inputs		Outputs	
	u_1	u_2	ψ [°]	φ [°]
Oper. range	[0, 0.6]	[−0.3, 0.3]	[−45, 45]	[−130, 130]

Considering the forces (torques) in the vertical plane, the elevation dynamics can be described by the following equations [16]:

$$
\begin{aligned}
a_\psi \ddot{\psi} &= \tau_1 + \tau_{\dot{\varphi}} - \tau_{f_1} - \tau_m + \tau_G, && (1)\\
\tau_m &= mgl \sin\psi, && (2)\\
\tau_{\dot{\varphi}} &= ml\dot{\varphi}^2 \sin\psi \cos\psi, && (3)\\
\tau_{f_1} &= C_\psi \text{sign}\, \dot{\psi} + B_\psi \dot{\psi}, && (4)\\
\tau_G &= k_G \dot{\varphi} \omega_1 \cos\psi, \text{ for } \dot{\varphi} \ll \omega_1, && (5)
\end{aligned}
$$

where:

a_ψ – moment of inertia around horizontal axis,
τ_1 – moment produced by the main motor propeller,
$\tau_{\dot{\varphi}}$ – centrifugal torque,
τ_{f_1} – Coulumb and viscous friction torques,
τ_m – gravitation torque,
τ_G – gyroscopic torque,
m – mass of the helicopter body,
g – gravitational acceleration,
l – distance from $z$axis to main motor axis,
ω_1 – angular velocity of the main propeller,
k_G – gyroscopic coefficient,
B_ψ – viscous friction coefficient,
C_ψ – Coulumb friction coefficient.

Taking into account the forces (torques) in the horizontal plane, the azimuth dynamics model can be taken as [16]:

$$
\begin{aligned}
a_\varphi \ddot{\varphi} &= \tau_2 - \tau_{f_2} - \tau_r, && (6)\\
\tau_{f_2} &= C_\varphi \text{sign}\, \dot{\varphi} + B_\varphi \dot{\varphi}, && (7)\\
a_\varphi &= a_\psi \sin\psi. && (8)
\end{aligned}
$$

where:

a_φ – moment of inertia around vertical axis,
τ_2 – moment produced by the side motor propeller,
τ_{f_2} – Coulumb and viscous friction torques,
τ_r – reaction torque of the main motor,
ω_2 – angular velocity of the side propeller,
B_φ – viscous friction coefficient,
C_φ – Coulumb friction coefficient.

B. Model of DC motors

It is impossible to directly identify physical parameters of DC motors due to helicopter body structure. Hence, no appropriate internal signal are available for measurements. Dynamics of the main motor model can be described as the second order transfer function [16]:

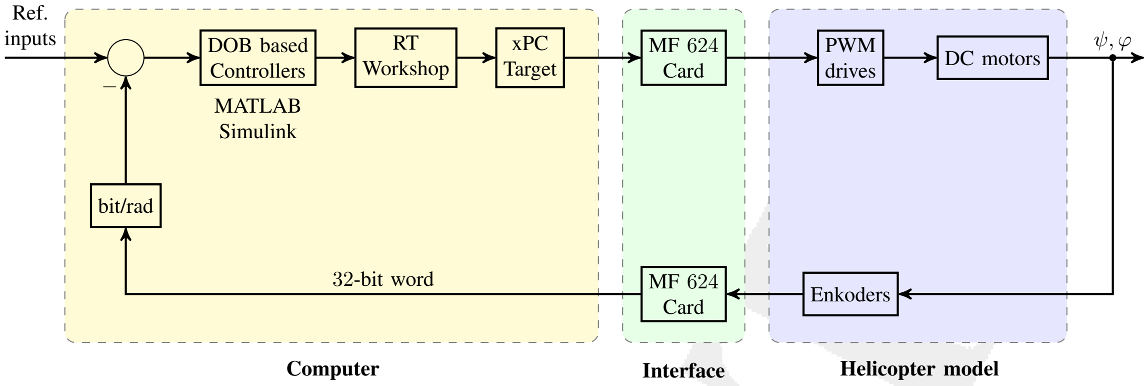

Fig. 1. Block diagram of the proposed real-time control system for the helicopter model

$$\frac{\omega_1(s)}{u_1(s)} = \frac{1}{(T_1 s + 1)^2}\,, \tag{9}$$

where $\omega_1(s)$ and $u_1(s)$ are Laplace transforms of $\omega_1(t)$ and $u_1(t)$ respectively, while T_1 is the main motor time constant. Torque generated by the main propeller can be presented with parabolic function of the angular velocity:

$$\tau_1(t) = a_1\omega_1^2(t) + b_1\omega_1(t). \tag{10}$$

The parameters that need to be considered in the identification process are: time constant T_1 and parameters of the propeller characteristic a_1 and b_1. Analogue relations as (9) and (10) can be defined for the side motors, but with parameters T_2, a_2, b_2.

C. DC motors cross-coupling model

One of the major characteristics of the helicopter are cross-coupling effects of the propellers. Exact identification of this reaction effects is not possible due to absence of appropriate signal measurements. Dynamics of the main motor reaction to the side motor can be described by the first order transfer function [16]:

$$\frac{\tau_r(s)}{u_1(s)} = K\frac{T_z s + 1}{T_p s + 1}\,. \tag{11}$$

An identification method presented in [16] requires specially prepared experiment for the determination of each individual helicopter parameter. For more accurate parameter identification each experiment needs to be repeated several times. In order to reduce the number of conducted experiments and simplify the process of identification, unknown helicopter parameters have been determined using a simple genetic algorithm [17]. Obtained values of helicopter parameters are shown in Table II.

TABLE II
PARAMETERS VALUE OF THE HELICOPTER MODEL CE 150

Parameter	Value	Unit
a_ψ	0.005435	$[\mathrm{kgm}^2]$
B_ψ	0.016	$[\mathrm{kgm}^2/\mathrm{s}]$
C_ψ	0.002	$[\mathrm{kgm}^2/\mathrm{s}]$
τ_g	0.071	$[\mathrm{Nm}]$
a_1	0.047	$[\mathrm{Nm}]$
b_1	0.089	$[\mathrm{Nm}]$
a_φ	0.002	$[\mathrm{kgm}^2]$
B_φ	0.006	$[\mathrm{kgm}^2/\mathrm{s}]$
C_φ	0.001	$[\mathrm{kgm}^2/\mathrm{s}]$
a_2	0.268	$[\mathrm{Nm}]$
b_2	0.0408	$[\mathrm{Nm}]$
K_G	0.0368	$[\mathrm{Nm/s}]$
K_c	0.0032	$[\mathrm{Nm/s}]$
K	0.0352	$[\mathrm{Nm}]$
T_z	2.7	$[\mathrm{s}]$
T_p	0.75	$[\mathrm{s}]$
T_1	0.1	$[\mathrm{s}]$
T_2	0.25	$[\mathrm{s}]$
K_ψ	0.167	$[^\circ]$
$y_{\psi 0}$	-45	$[^\circ]$
K_φ	0.176	$[^\circ]$

III. Synthesis of the DOB based Controller

For mechanical systems control task implies achieving the desired motion in dependence to the control input. In general, the main requirements to the control structure are: closed-loop system stability, tracking of the reference input, disturbance and noise effects reduction, parametric uncertainties reduction and unmodelled dynamics effect reduction.

Mathematical model of a single degree of freedom mechanical system (either translational or rotational) can be written in the following form [18]:

$$a_N\ddot{q}\,(t) + \tau_{dis}\,(q\,(t)\,, \dot{q}\,(t)\,, t) = \tau, \tag{12}$$

Here q and $\dot{q} \equiv v$ stands for the state variables, position and velocity, respectively; a_N is known nominal inertia coefficient and τ_{dis} is generalized input disturbance that includes Coriolis forces, friction force, gravitational forces, external forces (interaction forces - if contact with environment exists) and changes of the system parameter (i.e. variations of the system inertia $\Delta a(q)$). The elevation dynamics (2) can be described with (12), using identities: $a_N \equiv a_\psi$, $q \equiv \psi$, $\tau_{dis} \equiv \tau_{f1} + \tau_m - \tau_{\dot{\varphi}} - \tau_G$ and $\tau \equiv \tau_1$. Also, the azimuth dynamics (7) can be presented with (12), assuming:

$a_N \equiv a_\varphi$, $q \equiv \varphi$, $\tau_{dis} \equiv \tau_{f2} + \tau_r$ and $\tau \equiv \tau_2$.

The main idea consists in forming the control law as follows:

$$\tau = a_N \ddot{q}_{des} + \hat{\tau}_{dis}. \tag{13}$$

Applied force has two components, the estimated disturbance $\hat{\tau}_{dis}$ in the inner control loop and the force induced by desired torque $a_N \ddot{q}_{des}$ in the outer control loop. The control force (13) cancels plant input disturbance and makes plant a simple double integrator $\ddot{q} = \ddot{q}_{des}$, thus, robust in changes of system parameters and external forces. Implementation of control input (13) is shown in Fig. 2.

A. Synthesis of the outer control loop

In case the control output is linear or nonlinear continuous function of position $y(q)$, tracking error $e = y(q) - y_{ref}$ can be defined as a measure of the distance from reference value described by equilibrium solution. If tracking error is equal to zero, system output is constrained to domain or manifold:

$$S(q, \dot{q}) = \left\{ q \middle| \, e(q) = y(q) - y_{ref} = 0 \right\}. \tag{14}$$

Control task can be formulated as requirement to enforce equilibrium $e(y, y_{ref}) = 0$, or to enforce convergence to the manifold (14) and achieve stability of the equilibrium. Dynamics of the control error can be described using generalized error function σ:

$$\sigma = \sigma\left(e, \dot{e}\right) = \dot{e} + k_1 e, \tag{15}$$

where k_1 is a positive constant. Generalized error σ is selected to have relative degree one with respect to control input. Now, the desired acceleration $\ddot{q}_{des}$ needs to be selected to enforce output convergence and stability of equilibrium. Desired acceleration is composed of two components. The first one, called equivalent acceleration $\ddot{q}_{eq}$, stands for the value of the input acceleration for which the rate of change of the distance from the equilibrium is zero $\sigma = 0$. The second one, called convergence acceleration, is selected to guaranty convergence to equilibrium solution if initial conditions are not consistent with equilibrium $\sigma|_{t=0} \neq 0$ [18].

Dynamics of (15) can be expressed as follows:

$$\begin{aligned} \dot{\sigma} &= \ddot{e} + k_1 \dot{e} \\ &= \frac{\partial^2 y(q)}{\partial q^2} \dot{q}^2 + \frac{\partial y(q)}{\partial q} \ddot{q} - \ddot{y}_{ref} + k_1 \dot{e} \\ &= \frac{\partial y(q)}{\partial q} \left[\ddot{q} - \left(\frac{\partial y(q)}{\partial q} \right)^{-1} \left(\ddot{y}_{ref} - \frac{\partial^2 y(q)}{\partial q^2} \dot{q}^2 - k_1 \dot{e} \right) \right]. \end{aligned} \tag{16}$$

Now, desired acceleration can be derived from (16) in the form:

$$\ddot{q}_{des} = \ddot{q}_{eq} + \ddot{q}_{conv}, \tag{17}$$

$$\ddot{q}_{conv} = \left(\frac{\partial y(q)}{\partial q} \right)^{-1} \dot{\sigma}. \tag{18}$$

Equivalent acceleration yields from $\dot{\sigma} = 0$ and (16):

$$\ddot{q}_{eq} = \left(\frac{\partial y(q)}{\partial q} \right)^{-1} \left(\ddot{y}_{ref} - \frac{\partial^2 y(q)}{\partial q^2} \dot{q}^2 - k_1 \dot{e} \right). \tag{19}$$

To complete design of desired acceleration, the rate of change of the generalized error $\dot{\sigma}$ needs to be determined. For this purpose, Lyapunov function candidate can be selected as:

$$V = \frac{\sigma^2}{2} > 0, \, V(0) = 0. \tag{20}$$

The first order time derivative of (20) is:

$$\dot{V} = \sigma \dot{\sigma} = -2kV, \tag{21}$$

where k is a positive constant that represent Lyapunov convergence coefficient.

Relations (21) yields:

$$\dot{\sigma} + k\sigma = 0. \tag{22}$$

Solution of the (22) is exponentially decreasing function $\sigma(t) = \sigma(0) e^{-kt}$. This implies convergence to the equilibrium solution σ and the stability of the equilibrium. Now convergence acceleration can be determined as:

$$\ddot{q}_{conv} = -k \left(\frac{\partial y(q)}{\partial q} \right)^{-1} \sigma. \tag{23}$$

For the purpose of helicopter control, position (elevation or azimuth angle) is selected for output variable, i.e. $y(q) = q$. Finally, desired acceleration for the outer control loop can be formed using (19) and (23):

$$\ddot{q}_{des} = \ddot{y}_{ref} - \left(k_1 + k\right) \dot{e} - k k_1 e. \tag{24}$$

Obtained controller (24) consists of a PD control term in order to reduce computational burden, and a feed-forward control of a simple predictor to improve performances. Controller parameters k and k_1 are designed according to the nominal system $P_n(s) = 1/s^2$ that represents a simple double integrator. The coefficients $k_\psi = 4$ and $k_\varphi = 5$ are applied, so the elevation and azimuth angles tend to reference as quickly as possible. Also, the coefficients $k_{1\psi} = 6$ and $k_{1\varphi} = 20$ are applied, so the elevation and azimuth steady state errors are as small as possible.

B. Synthesis of the inner control loop

This subsection introduces design of the disturbance observer based on position measurements and known control force. Disturbance is defined as a sum of all possible signals due to the differences between the actual system and the model. This means that the actual plant with the disturbance compensator can be regarded as nominal model if the disturbance is well cancelled [14]. DOB based controller makes a system robust using Q-filter which cuts off the disturbance in low frequency range.

The augmented system (12) with model of disturbance $\dot{\vartheta} = \dot{\tau}_{dis} \approx 0$, $\vartheta = -a_N^{-1} \tau_{dis}$ is observable [18]. Intermediate variables can be selected as:

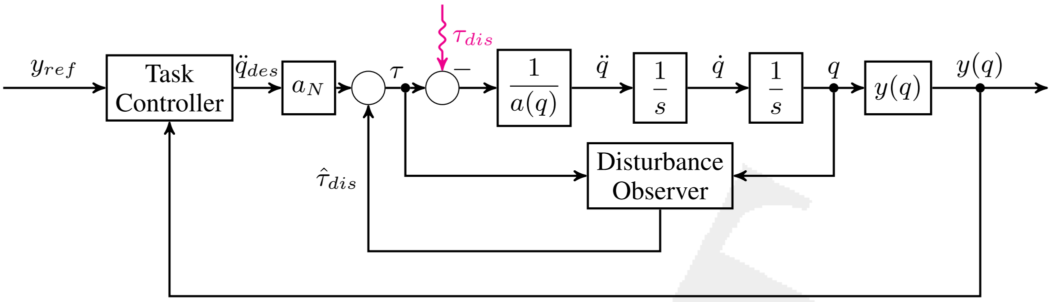

Fig. 2. Cascade control loop with DOB in the inner and task controller in the outer loop

$$z_1 = \vartheta - l_1 q,\ l_1 = const, \tag{25}$$
$$z_2 = v - l_2 q,\ l_2 = const. \tag{26}$$

The first order time derivation along the trajectories of system (12) are:

$$\dot{z}_1 = -l_1 \left(z_2 + l_2 q\right), \tag{27}$$
$$\dot{z}_2 = z_1 - l_2 z_2 + \left(l_1 - l_2^2\right) q + a_N^{-1} \tau. \tag{28}$$

The dynamics of the observer should be the same as dynamics of the intermediate variables and can be written as:

$$\dot{\hat{z}}_1 = -l_1 \left(\hat{z}_2 + l_2 q\right), \tag{29}$$
$$\dot{\hat{z}}_2 = \hat{z}_1 - l_2 \hat{z}_2 + \left(l_1 - l_2^2\right) q + a_N^{-1} \tau. \tag{30}$$

Solving for $\hat{z}_1$ Laplace transformation of (29) and (30) yields:

$$\hat{z}_1 = -l_1 \frac{l_2 s q + l_1 q + a_N^{-1} \tau}{s^2 + l_2 s + l_1}. \tag{31}$$

Substituting (31) into $\hat{\vartheta} = \hat{z}_1 + l_1 q$, it can be written:

$$\hat{\tau}_{dis} = \frac{l_1}{s^2 + l_2 s + l_1} \tau_{dis}. \tag{32}$$

The pole position of the observer α and β are determined by constants l_1 and l_2:

$$\alpha + \beta = -l_2, \tag{33}$$
$$\alpha\beta = l_1. \tag{34}$$

Implementation of the disturbance observer (32) is shown in Fig. 3. Poles position $l_{1\psi} = 0.6$, $l_{2\psi} = 1.7$ are selected for the elevation dynamics, and $l_{1\varphi} = 1.2$, $l_{2\varphi} = 1.7$ for the azimuth dynamics, so the observer could estimate disturbance in a low frequency and noise in a high frequency range.

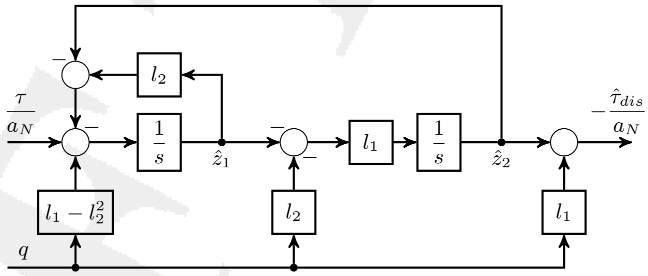

Fig. 3. Disturbance observer with the position and the force as inputs

IV. Simulation and Experimental Results

In this section, the simulation and the experimental results of the helicopter CE 150 control are presented. A Simulink model of the helicopter system was developed for the simulations according to section II. If the DOB based controllers estimate and attenuate cross-coupling effects and generalized disturbance as well, the complex helicopter system can be treated like set of two SISO systems. Consequently, the synthesis of the DOB based controller of the elevation dynamics is performed independently to the azimuth dynamics (according to the section III), and vice versa.

A. Simulation results

This subsection presents the effectiveness of the DOB based controllers in comparison to the fuzzy controllers proposed in [6]. Elevation angle responses are shown in Fig. 4 and azimuth angle responses in Fig. 5. Changes of the elevation and azimuth reference values are simultaneous in all conducted experiments. It can be noticed in Fig. 4 that DOB based controller can achieve better tracking performance over the wide range of elevation angles with lower overshoots and steady state errors. Moreover, the steady state error of the elevation angle with DOB controller is exponentially decreasing, while fuzzy controller provides errors depending to the operation range. In Fig. 5 there are obvious higher oscillations at the azimuth response based on the fuzzy controller. This implies more power consumption and higher strain rates of the DC motor.

B. Experimental results

In this subsection, the improvements of the DOB based control system are presented through experiments. In the

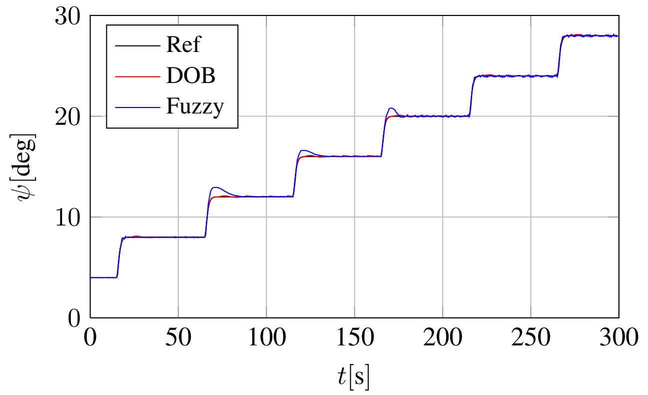

Fig. 4. Comparison of the elevation angle responses at the simulation mode

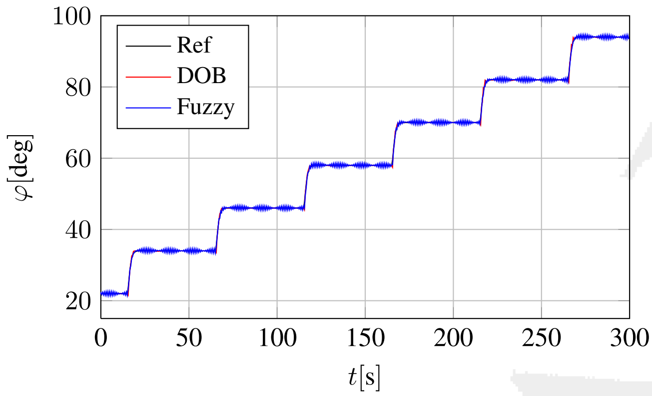

Fig. 5. Comparison of the azimuth angle responses at the simulation mode

Fig. 6 it can be seen that DOB based controller is capable to eliminate influence of the azimuth angle. The fuzzy controller provides poor tracking of the elevation angle at the moments of high changes in the azimuth reference signal. Fig. 7 shows significant improvements of the DOB based azimuth output without high overshoots. In the Fig. 8 control errors are presented. The DOB based control error in the steady state is about 1.5%. Most important feature of the DOB control is shown in the Fig. 9. Power consumption and main motor strains with DOB control are significantly less comparing to the fuzzy control.

V. Conclusions

In this paper disturbance observer based controllers are designed and implemented to the nonlinear helicopter system CE 150. Proposed DOB based controllers guarantee robust and stable closed-loop behaviour of the helicopter body for a wide range of azimuth and elevation angles during the long time flight. Designed disturbance observer based controllers compensate severe nonlinear friction in the bearings, uncertainties of the system parameters, unmodelled dynamics, external disturbances and strong interactions of the elevation and azimuth dynamics. Proposed controllers consist of a PD feedback control in order to reduce computational burden, a disturbance observer to estimate uncertainties and a feed-forward control of a simple predictor to improve performances. Implementation of the DOB based controllers is very simple despite the need for relatively short sampling time combined with substantial controller computation. It is shown that designed controller uses less power and improves tracking performance. The validity of the proposed cascade control structure was verified through both, simulation and experiment.

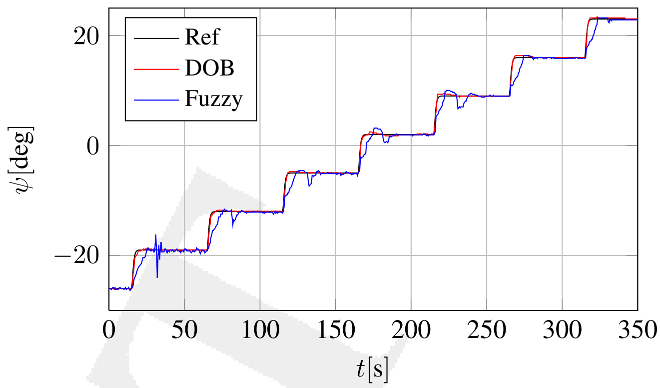

Fig. 6. Comparison of the elevation angle responses at the experimental setup

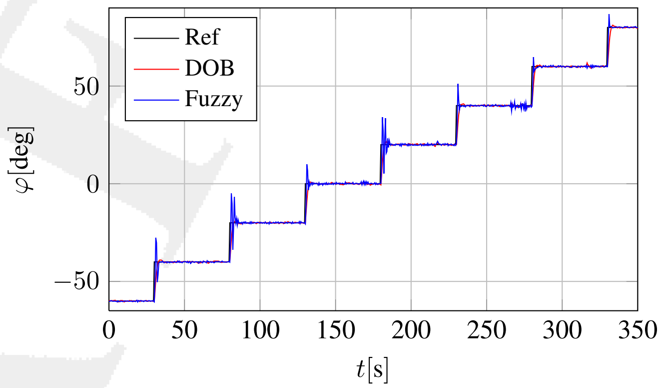

Fig. 7. Comparison of the azimuth angle responses at the experimental setup

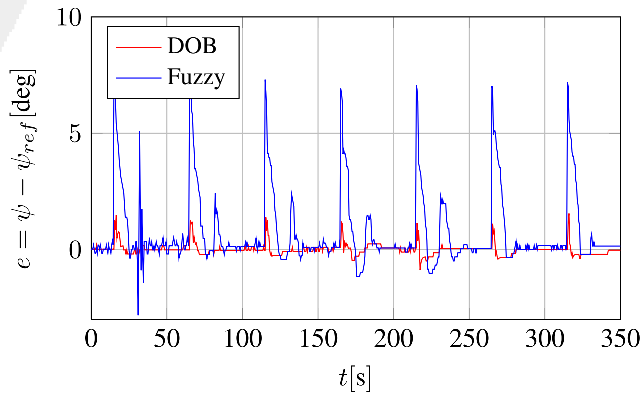

Fig. 8. Comparison of the control error for the elevation angle

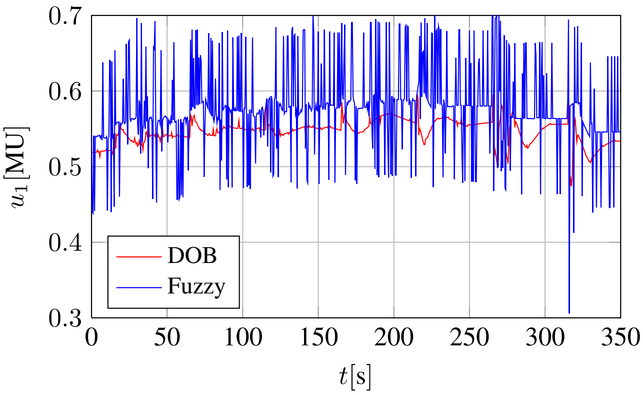

Fig. 9. Comparison of the control input for the elevation angle

References

[1] A. Isidori and C. I. Byrnes, "Output regulation of nonlinear systems," in *IEEE Transactions on Automatic Control*, vol. 35, no. 2, Feb. 1990, pp. 131–140.

[2] T. J. Koo and S. Sastry, "Output tracking control design of a helicopter model based on approximate linearization," in *Proceedings of the 37th IEEE Conference on Decision and Control*, vol. 4, Dec. 1998, pp. 3635–3640.

[3] C. Tomlin, J. Lygeros, L. Benvenuti, and S. Sastry, "Output tracking for a non-minimum phase dynamic ctol aircraft model," in *Proceedings of the 34th IEEE Conference on Decision and Control*, vol. 2, Dec. 1995, pp. 1867–1872.

[4] H. L. Pei, Y. Hu, and Y. Wu, "Gain scheduling control of a small unmanned helicopter," in *IEEE International Conference on Control and Automation*, 2007, pp. 1168–1173.

[5] J. Velagic and N. Osmic, "Design and implementation of fuzzy logic controllers for helicopter elevation and azimuth controls," in *IEEE Conference on Control and Fault Tolerant Systems*, Nice, France, Oct 2010, pp. 311–316.

[6] J. Velagic, N. Osmic, T. Uzunovic, A. Badnjevic, and E. Zunic, "Neural networks for helicopter azimuth and elevation angles control obtained by cloning processes," in *IEEE System, Man and Cybernetics Conference*, Istanbul, Turkey, Oct 2010, pp. 1076–1082.

[7] J. Velagić and N. Osmić, "Identification and control of 2dof nonlinear helicopter using intelligent methods," in *IEEE Conference on System, Man and Cybernetics*, Istanbul, Turkey, 2010, pp. 2267–2275.

[8] J. Balderud and D. I. Wilson, "A comparison of optimal control strategies for a toy helicopter," in *Asian Control Conference*, Singapore, Sep 2002, pp. 1432 – 1437.

[9] ——, "Application of predictive control to a toy helicopter," in *IEEE International Conference on Control Applications*, Glasgow, Scotland, Sep 2002, pp. 1225–1229.

[10] M. Nakao, K. Ohnishi, and K. Miyachi, "A robust decentralized joint control based on interference estimation," in *IEEE International Conference on Robotics and Automation*, 1987, pp. 326–331.

[11] X. Chen, S. Komada, and T. Fukuda, "Design of nonlinear disturbance observer," in *IEEE Transactions on Industrial Electronics*, vol. 47, 2000, pp. 429–437.

[12] H. S. Lee and M. Tomizuka, "Robust motion controller design for high accuracy positioning systems," in *IEEE Transactions on Industrial Electronics*, vol. 43, 1996, pp. 48–55.

[13] C. J. Kempf and S. Kobayashi, "Disturbance observer and feedforward design for a high-speed direct-drive positioning table," in *IEEE Transactions on Control System Technology*, vol. 7, 1999, pp. 513–526.

[14] B. K. Kim and W. K. Chung, "Advanced design of disturbance observer for high performance motion control systems," in *American Control Conference*, 2002, pp. 2112–2117.

[15] M. White, M. Tomizuka, and C. Smith, "Rejection of disk drive vibration and shock disturbances with a disturbance observer," in *IEEE American Control Conference*, vol. 6, 1999, pp. 4127 – 4131.

[16] P. Horáček, *CE 150 HELICOPTER MODEL, Educational manual*, Humosoft Ltd., Czech Republic, 2007.

[17] N. Osmic, J. Velagic, and S. Konjicija, "Genetic algorithm based identification of a nonlinear 2dof helicopter model," in *IEEE Mediterranean Conference on Control and Automation*, Marrakech, Morocco, 2010, pp. 333–338.

[18] A. Šabanović and K. Ohnishi, *Motion control systems*. Chichester, United Kingdom: Wiley & Sons, Ltd, 2011.